SPIN BLOCKADES IN ELECTRON TRANSPORT

DIETMAR WEINMANN*, WOLFGANG HÄUSLER,
KRISTIAN JAUREGUI AND BERNHARD KRAMER
Universität Hamburg, I. Institut für Theoretische Physik, Jungiusstr. 9, 20355 Hamburg, F. R. G.

Abstract. Linear and non–linear transport through a quantum dot weakly coupled to leads is investigated in the regime where charging and geometrical quantization effects are important. A master equation is combined with the exact quantum states of a finite number of strongly correlated electrons with spin inside the dot. The current–voltage characteristic of a quasi–one dimensional dot shows Coulomb blockade and additional finestructure that is related to the excited states of the electrons. Negative differential conductances occur due to spin selection rules that can lead to a 'spin blockade' which, in contrast to the Coulomb blockade, even reduces the current when the transport voltage is increased. In two dimensional dots spin effects can suppress linear conductance peaks at low temperatures.

1. Introduction

Using recent nanostructure fabrication techniques one can make samples in which electrons are confined to very small regions in space, so–called quantum dots. They can be considered as 'artificial atoms' [1] with tunable parameters, and allow to study systematically a few interacting electrons. While correlations are very difficult to observe in infrared absorption spectroscopy, the spectrum of the interacting electrons can be investigated in great detail by using non–linear transport. When the quantum dot and the external reservoirs are only weakly coupled, transport is dominated by the dot. If the latter is small enough, the charging energy E_C needed to add a single electron can exceed the thermal energy $k_B T$ at low temperature.

*on leave from Universität Stuttgart, II. Institut für Theoretische Physik, Pfaffenwaldring 57, 70550 Stuttgart, F. R. G.

This leads to the suppression of the conductance known as the Coulomb blockade effect [2].

The current is blocked if $\mu_L \approx \mu_R \neq E_0(n) - E_0(n-1)$, where $\mu_{L/R}$ is the chemical potential in the left/right lead and $E_0(n)$ the ground state (GS) energy of n electrons. On the other hand, if $\mu_L \approx \mu_R = E_0(n) - E_0(n-1)$, the number of electrons inside the dot can oscillate between n and $n-1$ (single electron tunneling (SET) oscillations), and the conductance is finite. The resulting peaks of the conductance as a function of the carrier density are experimentally well established [3]. They can be observed if the coupling to the leads (characterized by the tunneling resistance R_T) is weak enough, $R_T \gg h/e^2$, to avoid quantum smearing and therefore guaranteeing n to be a good quantum number on a sufficiently long time scale.

In semiconductor quantum dots, the electron density is considerably lower than in metallic systems and the excitation energies $\Delta\varepsilon$ for a fixed number of electrons can exceed $k_B T$ at mK–temperatures. At transport voltages $V > \Delta\varepsilon$, characteristic splittings of the conductance peaks occur. The current–voltage characteristic shows fine structure in addition to the Coulomb steps [4, 5, 6, 7, 8, 9, 10, 11, 12]. We shall demonstrate that this is related to the excited states of the quantum dot and allows to investigate experimentally the spectrum of their energy levels [4, 5, 12].

However, the current does not necessarily increase when, by raising V, the number of possible transitions between n and $n-1$ electron states is raised. Spin selection rules can suppress certain transitions and reduce the current if the electrons in the dot are spin–polarized such that the total spin $S = n/2$. Then, the electron number can only be decreased by simultaneously reducing the total spin [13]. Regions of negative differential conductance (NDC) occur due to a 'spin blockade' [13, 14, 15, 17]. Such regions have been observed in experiment [5, 6].

We consider quasi–one dimensional(1D) and 2D square quantum dots in order to investigate the influence of dimensionality on this novel blockade mechanism. The spectra of the different models are qualitatively different. NDCs occur in 1D systems at high V, of the order of the excitation energy of the spin–polarized state. For the square dots we present results which are associated with low lying excited states that do not necessarily have maximum spin. We show that even in linear transport the current may be suppressed by spin effects, namely if the total spins of the GSs of successive electron numbers differ by more than $\pm 1/2$. NDCs can occur close to a conductance peak even at very low V if an excited state with large (not necessarily maximum) total spin lies energetically close to the GS. We demonstrate that this leads to interesting temperature and V dependencies of the conductance peaks.

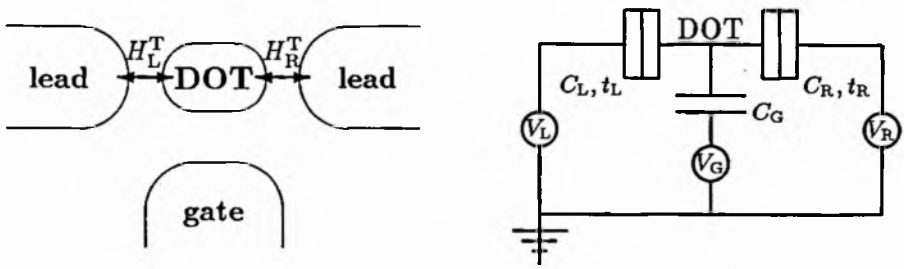

Figure 1. Left: scheme of the quantum dot, left/right leads, and gate electrode. Tunnel junctions are modeled by $H^T_{L/R}$. Right: equivalent circuit.

2. Model

As a model for a dot, weakly connected to leads (Fig. 1), we consider the Hamiltonian $H = H_D + H_L + H_R + H_L^T + H_R^T$, where $H_{L/R} = \sum_{k,\sigma} \varepsilon_k^{L/R} c^+_{L/R,k,\sigma} c_{L/R,k,\sigma}$ describes free electrons in the left/right lead. They are assumed to be large and in thermal equilibrium. The Hamiltonian for interacting electrons with spin $\sigma = \pm 1/2$ in the dot is

$$H_D = \sum_{l,\sigma} (\varepsilon_l - e\Phi) c^+_{l,\sigma} c_{l,\sigma} + \sum_{\substack{l_1,l_2,l_3,l_4 \\ \sigma_1,\sigma_2,}} V_{l_1 l_2 l_3 l_4}\, c^+_{l_1,\sigma_1} c^+_{l_2,\sigma_2} c_{l_3,\sigma_2} c_{l_4,\sigma_1} \,. \qquad (1)$$

The energies of the non–interacting electrons are ε_l and $V_{l_1 l_2 l_3 l_4}$ the matrix elements of the Coulomb interaction. An equivalent circuit from which we find the potential change Φ in the dot due to the gate voltage V_G and the transport voltages is sketched in Fig. 1. It appears to be a realistic model for experiments [4].

Furthermore, we assume that the phase coherence of the eigenstates of H is destroyed on a time scale $\tau_\varphi \gg h/\Delta\varepsilon$ [1]. Thus, the broadening of the quasi–discrete levels inside the dot due to phase breaking is negligible.

The tunneling terms $H^T_{L/R} = \sum_{k,l,\sigma} \left(T^{L/R}_{k,l} c^+_{L/R,k,\sigma} c_{l,\sigma} + h.c. \right)$ represent the barriers. We assume the transmission probability amplitudes $T^{L/R}_{k,l}$ to be independent of k, l and σ, and the tunneling rates $t_{L/R} = (2\pi/\hbar) \sum_{k,\sigma} \left| T^{L/R}_{k,l} \right|^2 \delta(\varepsilon^{L/R}_k - E)$ to be independent of the energy E. If the latter are small as compared to the phase breaking rate τ_φ^{-1}, the time evolution of the occupation probabilities of the many–electron states in the dot can be calculated using a master equation.

[1] It is well known that strong dissipation can suppress tunneling (see e. g. [18]). This choice for the phase breaking rate τ_φ^{-1} guarantees that the renormalization of the tunneling rates through the barriers is negligible.

3. Method

The transport is determined by transitions between eigenstates of the isolated dot that correspond to different electron numbers. These transitions are due to electrons which tunnel between the leads and the dot.

First, we determine the many–electron eigenstates $|\Psi_i^{\mathrm{D}}\rangle$ and the corresponding eigenenergies E_i of H_{D}. Then, we calculate the transition rates between these states to lowest order in $H_{\mathrm{T}}^{\mathrm{L/R}}$. Due to the smallness of H^{T}, simultaneous transitions of two or more electrons [22], processes of higher order, are strongly suppressed. Fermi's golden rule yields for the rates

$$\begin{aligned}\Gamma_{ji}^{\mathrm{L/R}} &= \frac{1}{2}\left|\langle S_i, M_i, \frac{1}{2}, \pm\frac{1}{2} \mid S_j, M_j\rangle_{CG}\right|^2 t_{\mathrm{L/R}} \\ &\times \left(f_{\mathrm{L/R}}(E)\delta_{n_j,n_i+1} + [1 - f_{\mathrm{L/R}}(-E)]\delta_{n_j,n_i-1}\right)\end{aligned} \tag{2}$$

for $|\Psi_i^{\mathrm{D}}\rangle \rightarrow |\Psi_j^{\mathrm{D}}\rangle$. The electron has to provide the energy difference $E = E_j - E_i$. The transition matrix elements are assumed to be given by the Clebsch–Gordan coefficients $\langle\ldots\rangle_{CG}$, which arise from the spin. They introduce spin selection rules. Rates vanish between states when the differences between their total spins S or their magnetic quantum numbers M are not $\pm 1/2$.

With the total transition rates $\Gamma = \Gamma^{\mathrm{L}} + \Gamma^{\mathrm{R}}$, we can write the master equation for the time evolution of the occupation probabilities P_i of the many–electron dot states

$$\frac{d}{dt}P_i = \sum_{j\,(j\neq i)} (\Gamma_{ij}P_j - \Gamma_{ji}P_i) \qquad \text{with} \qquad \sum_i P_i = 1\,. \tag{3}$$

Assuming $dP/dt = 0$, and solving the resulting linear system (3), one gets the stationary non–equilibrium populations $\bar{P}_i$ for arbitrary V without further restrictions.

At $V = 0$, the stationary state is the equilibrium state. The populations of the n–electron states are given by a Gibbs distribution $P_i^{\mathrm{G}} = (\exp[-\beta(E_i - \mu n_i)])/\mathcal{Z}$ with the chemical potential $\mu = \mu_{\mathrm{L}} = \mu_{\mathrm{R}}$ and the grand canonical partition function $\mathcal{Z}$. For temperatures lower and voltages higher than the level spacings, $\bar{P}_i$ deviate from P_i^{G} [14, 20].

Finally, one determines the dc–current by considering one of the barriers,

$$I \equiv I^{\mathrm{L/R}} = (-/+)e \sum_{i,j\,(j\neq i)} \bar{P}_j \Gamma_{ij}^{\mathrm{L/R}}(n_i - n_j)\,. \tag{4}$$

A similar method was used in the FQHE regime without spin [19]. It was also applied to the spinless phenomenological charging model [14, 20, 21].

The current–voltage characteristic shows finestructure in addition to the Coulomb steps. However, the NDCs observed in the experiments [5, 6] cannot be explained within the charging model.

In contrast to [21], where changes in the occupation probabilities of one–electron levels were considered, we take into account the $\bar{P}_i$ of all possible many–electron Fock states $|\ \Psi_i^{\mathrm{D}}\rangle$ of H_{D}. This allows to investigate the influence of the quantum properties on the transport beyond the charging model, and to discuss the influence of the electron spin.

4. Correlated electrons in quasi–one dimension

4.1. DOT SPECTRUM

We consider now n electrons in a quasi–(1D) well of length L [13, 14] including spin. For this system, numerical results for $n \leq 4$ [23], and analytical results [24] for the lowest excitations for low charge density exist. The interaction potential was assumed as $V(x,x') \propto ((x-x')^2+\lambda^2)^{-1/2}$. The cutoff λ ($\ll L$) is due to a lateral spread of the wave functions.

The correlated states and the energy spectra were discussed in detail [23]. For not too large electron densities the charge distribution in the dot has n distinct peaks indicating Wigner crystallization [25]. The electrons form a 'Wigner molecule'. The excitation spectrum consists of well separated multiplets, each containing 2^n states. The energetic differences between adjacent multiplets decrease algebraically with electron density. They correspond to vibrational excitations. The considerably smaller intra–multiplet energy differences decrease exponentially. They are due to correlated tunneling between different configurations of the n electrons. The wave functions of individual levels within a given multiplet differ in symmetry and S.

We take into account all the states in the lowest multiplets. The energetic order of the states with different spins is strongly influenced by the interaction and the geometry of the quantum dot. Together with the spin selection rules it leads to qualitatively new effects in the transport properties. In addition to the Coulomb blockade, further, purely quantum mechanical blocking mechanisms occur, as will be discussed in the following.

4.2. SPIN BLOCKADE TYPE I

The current–voltage characteristic is shown in Fig. 2(left). The most striking correlation effects are the NDCs [13, 14, 15, 16]. They are related to the fact that the states with maximum spin, $S = n/2$, can only decay into states of lower electron number when S is reduced by $1/2$. For a more detailed understanding, we focus attention to the NDC in the third conductance peak,

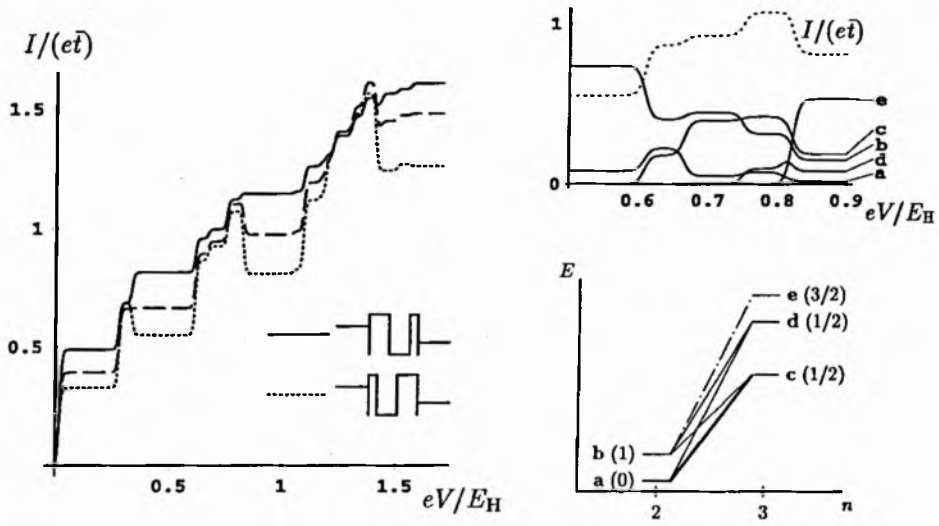

Figure 2. Left: current–voltage characteristic ($\mu_R = 0$, $\Phi = 0$) of a dot for inverse temperature $\beta = 200/E_H$. Dashed, dotted and solid lines correspond to $t_R/t_L = 1$, 0.5 and 2. Current is given in units of $\bar{t} = t_L t_R/(t_L t_R)$. Right top: most prominent feature for $t_L > t_R$. Current (dotted) and populations of the most relevant dot states are shown. Populations do not sum up to unity due to the occupation of other states. Right bottom: dot states for $n = 2$ and $n = 3$. The corresponding total spins S and allowed transitions are indicated. In linear transport, only GS–GS transition (thick line) contributes. At finite V, additional transitions between excited states contribute. Since the transition to the highest state (dotted–dashed) is a 'dead end', the current is reduced when e is populated.

near $eV/E_H = 0.8$. The transport voltage is high enough to allow all of the transitions between the states with $0 \leq n \leq 2$. Finestructure steps occur when the voltage allows additional transitions between states with $n = 2$ and $n = 3$. By plotting the stationary occupation probabilities of the corresponding states together with the current as a function of V (Fig. 2(right top)), one observes that each step in the current is accompanied by changes in the populations of the corresponding n–electron states.

For a better understanding of the underlying physical mechanism, we consider the spin–allowed transitions between the energy levels for $n = 2$ and $n = 3$ (Fig. 2(right bottom)). While the 'exit' through the right barrier is always possible, 'entries' through the left barrier are opened one after the other by increasing $V = \mu_L/e$. At low $\mu_L = E_j - E_i$, only states with $n \leq 2$ can be occupied. As soon as the voltage is high enough ($eV/E_H \approx 0.6$) to allow for the $n = 2 \rightarrow 3$ transition with the lowest energy, $\mu_L = E_c - E_b$, state **c** becomes populated. At the next step, the GS–GS transition becomes possible. Then, at $eV/E_H \approx 0.75$, the transition from state **b** to **d** comes

into play. It populates the first excited n–electron state (**d**). All these steps are accompanied by increasing values of the current.

For $eV/E_H \approx 0.8$, the transition to the energetically highest state **e** becomes available. It attracts considerable stationary occupation probability at the expense of all the other populations and the current is decreased. Due to the spin selection rules the probability to leave the state **e** by lowering the electron number is reduced. Therefore, the lifetime of this state is exceptionally large. This leads to the high population and the reduction of the current because the total number of transitions per unit of time is decreased when **e** can be occupied. This 'spin blockade type I' [13] is related to states with maximum spin and with high energy within the lowest multiplets. In 1D, these occur only once in each multiplet for a given n. Therefore only one finestructure step with NDC can occur within each Coulomb step.

For asymmetric barriers, $t_L > t_R$ ($\mu_L > \mu_R$), transitions which decrease n are relatively slow. Thus, the transition into the 'dead end' **e** becomes almost a 'one way road'. The spin blockade is enhanced (Fig. 2). If, on the other hand, processes with decreasing n are fast ($t_L < t_R$), state **e** loses its trap–like property. The spin blockade is suppressed. Such a behavior of an NDC has been seen in experiment [5, 6] but certainly needs further investigations.

4.3. TRANSPORT SPECTROSCOPY

The current through a quantum dot is determined by transitions between all of the states, including excited ones. Electron–electron correlations are of crucial importance. Thus, non–linear transport experiments are a powerful tool to investigate confined interacting electrons [6, 12]. To gain deeper insight into the dependence of the conductance on the various parameters, we plot the differential conductance $\partial I/\partial V$ as a function of V and V_G.

4.3.1. *Energetically possible transitions*

Transitions between many–electron states $n_j = n_i + 1$ can contribute to the current if their energy difference $E = E_j - E_i$ satisfies $\min(\mu_L, \mu_R) < E < \max(\mu_L, \mu_R)$. At $T = 0$, $\partial I/\partial V$ can only be non–zero on lines in the V–V_G plane given by $\mu_L = E$ and $\mu_R = E$. We assume $\mu_L = 0$ and $eV = \mu_L - \mu_R = -\mu_R$. Using the dependence of the many–electron energies on Φ, i. e. on the voltages applied to the gate and the leads, one finds

$$\begin{aligned} \frac{e}{C_\Sigma}(C_G V_G + C_R V) &= E_0 \\ \frac{e}{C_\Sigma}(C_G V_G - (C_L + C_G)V) &= E_0\,, \end{aligned} \tag{5}$$

where $E_0 \equiv E(\Phi = 0)$ and $C_\Sigma = C_L + C_R + C_G$ is the total capacitance.

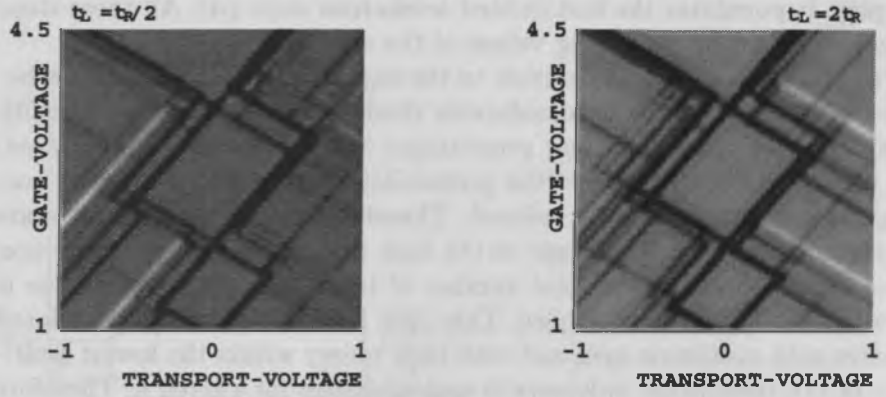

Figure 3. Grey–scale plot of the differential conductance versus V_G and V in units of E_H/e for $t_L = t_R/2$ (left) and $t_L = 2t_R$ (right). Zero conductance inside the grey diamond shaped regions centered around $V = 0$ is due to the Coulomb blockade. Dark and bright parts indicate positive and negative DCs, respectively. Bright regions occur mainly when the less transmitting barrier is attached to the lead with the lower of the chemical potentials.

The slopes of the lines (5) depend only on the properties of the circuit (ratios of the capacitances) while the position of the intersection with the V_G–axis is determined by the eigenvalues of the isolated dot and C_G. For simplicity, we use $C_L = C_R = C_G$.

4.3.2. *Differential conductance*

A grey–scale picture of the differential conductance is shown in Fig. 3. At $V = 0$ linear conductance peaks [3] (black regions) can be seen with diamond–shape regions of the Coulomb blockade in between. Lines that intersect at the positions of the peaks correspond to GS–GS transitions. Lines parallel to the edges of the Coulomb blockade areas reflect the dot spectrum [12, 15, 16]. Similar features were observed experimentally [6, 12].

When either V_G or V is changed, the populated states change. At $T = 0$, this leads to jumps in the current. Finite V broadens the conductance peaks, and leads to finestructure which reflects the dot spectrum. It is in general asymmetric [5, 10]. If the barriers are not equally transparent, the asymmetry is reversed when reversing V [14] consistent with experiment [7].

Fig. 3 shows results for different ratios of barrier transparencies. Transitions through the less transmitting barrier lead to more pronounced steps in the current, including the spin blockade. Bright regions correspond to NDCs. They are most pronounced when the lower chemical potential is attached to the less transmitting barrier, again consistent with experiment [12].

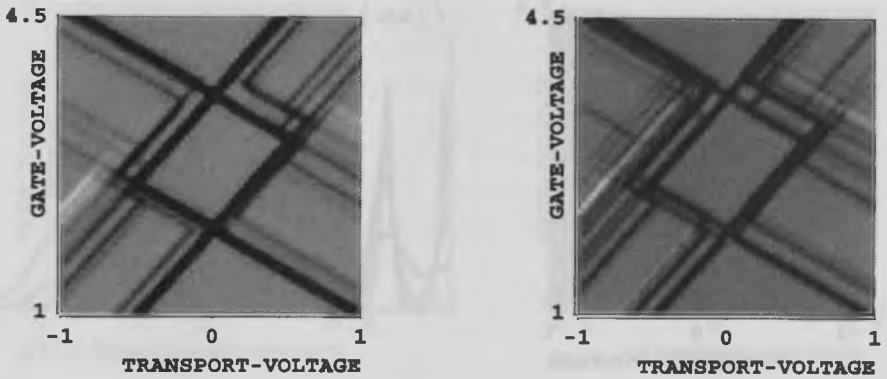

Figure 4. Differential conductance versus V and V_G in units of E_H/e at $t_L = t_R$ as obtained by using the full transition matrix elements (left), and by using only their spin part (right). Only states with 2, 3, and 4 electrons are taken into account.

4.4. THE INFLUENCE OF THE TRANSITION MATRIX ELEMENTS

Taking into account only the spin part of the transition matrix elements led to non–trivial blockade effects in the transport properties. The question remains, to what extend the spatial part of the wave functions would enhance or destroy these features. For the quasi–1D model, the transition matrix elements $\left|\sum_{l,\sigma}\langle\Psi_j^D \mid c_{l,\sigma}^+ \mid \Psi_i^D\rangle\right|^2$ between dot states of different electron number, which in general enter the transition rates (2), can be calculated numerically [26]. They reproduce the spin selection rules, as expected, in addition to providing information about the effect of the spatial part of the wave functions. For a regular barrier one can assume $T_{k,l} \equiv T$ in the tunneling Hamiltonian.

Fig. 4 shows that the influence of the spatial part of the wave functions generally reduces the structure in the DC by suppressing some of the transitions leaving, however, the qualitative features unchanged. In particular, no additional NDCs are introduced.

In contrast to the spin part, which represents a genuine quantum blockade effect, the spatial part of the matrix elements depends sensitively on the specific properties of the sample. In the example discussed above, there are strong fluctuations in the values for different transitions which suppress some of the transitions *in addition* to the spin selection rules. Such effects have been proposed in the framework of rotationally symmetric dots [27] in order to explain the low number of transitions observed in the experiments [6]. At present, the influence of the spatial part of the matrix elements is not yet fully investigated.

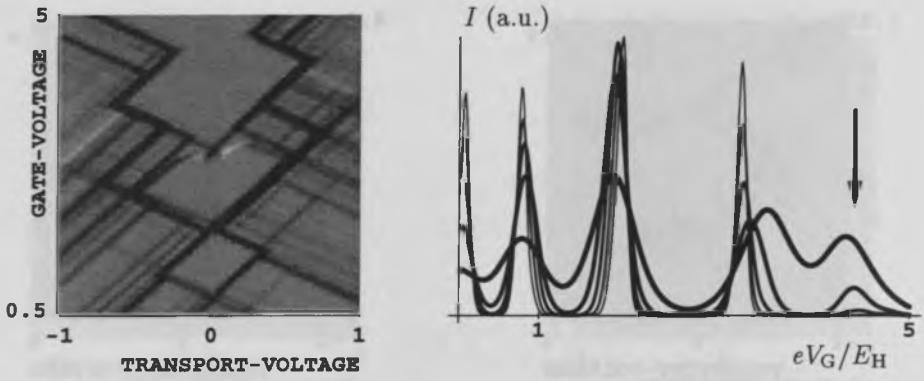

Figure 5. Left: differential conductance versus V_G and V in units of E_H/e of a square dot. Transition between the GSs for $n = 4$ and $n = 5$ is forbidden by the spin selection rule. Right: current versus V_G for increasing temperature, $\beta E_H = 100, 80, 60, 40, 20$ (increasing line thicknesses). The peak missing in linear conductance corresponds to oscillations between $n = 4$ and $n = 5$. It is recovered (arrow) by increasing T. The unusual shift of the peak with increasing T, corresponding to the transition between $n = 3$ and $n = 4$, is due to the weak GS–GS coupling is and induced by transport via excited levels when T increases.

5. Two–dimensional square dots

In order to investigate the geometry dependence of the spin blockade effect in more detail, we consider in this section square and rectangular quantum dots. In the low density regime the low energy excitations can again be calculated by using a correlated–tunneling model [24]. Results for up to five electrons are presently available. The spectrum is considerably different from its 1D counterpart. States with high spin occur close to the GS. The latter is not necessarily a state with minimum spin. This leads to additional blockade effects that are related to the spin of the electrons.

5.1. SPIN BLOCKADE TYPE II

As discussed above, the 'spin blockade type I' is related to the occupation of states with maximum spin, $S = n/2$. It appears at transport–voltages of the order of their excitation energies. They occur as excited states both in 1D [23] and in 2D [24] quantum dots.

The 'spin blockade type II' is related to states with high (not necessarily maximum) spin being GS or at least energetically close to the GS. Such situations can occur in 2D. If the total spins of the GSs that correspond to successive electron numbers differ by more than 1/2 the dot is blocked in the n– or the $n-1$–electron GS and the corresponding peak in the linear conductance is missing at $T = 0$.

Fig. 5(left) shows the differential conductance. A prominent feature is

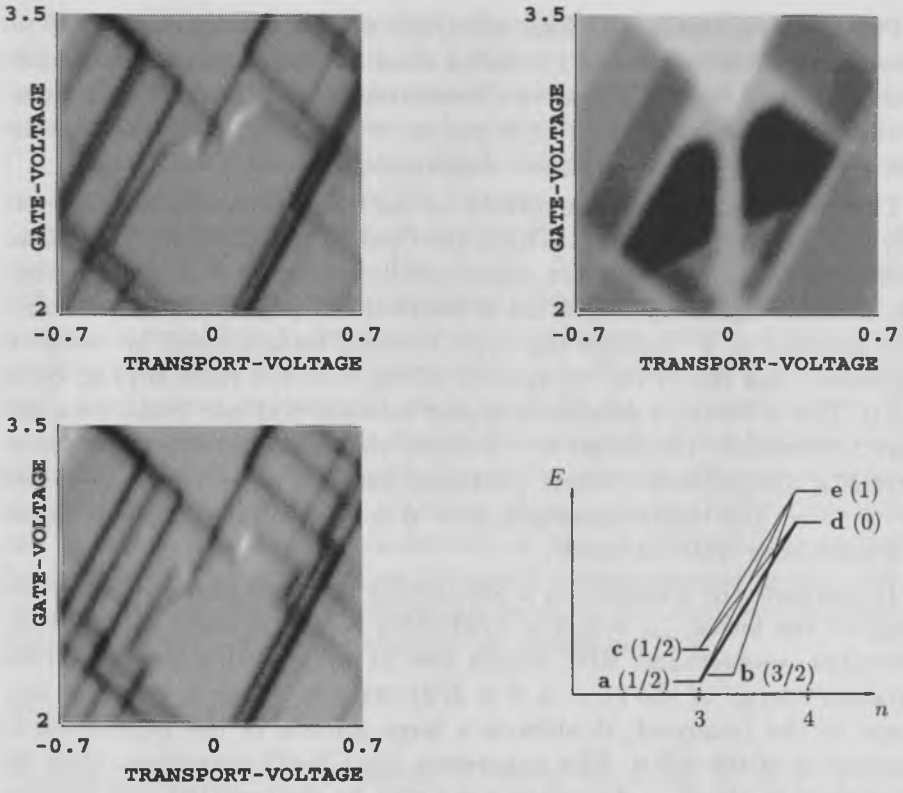

Figure 6. Top left: differential conductance near the transition between $n = 3$ and $n = 4$, and with the energy of the $S = 3/2$ state **b** close to the $(n = 3, S = 1/2)$–GS **a**. For small but finite V the state **b** becomes populated and transitions to the $n = 4$–GS are spin–forbidden. NDCs appear at low V. Top right: population of the $(n = 3, S = 3/2)$–state **b**. DArk regions correspond to high population. If V is high enough to occupy the state **b** it is easily populated, but depopulation is difficult. Bottom left: differential conductance with slightly increased energy of state **b**. The line corresponding to the GS–GS transition disappears at low V and is recovered at higher V. Bottom right: some dot states for $n = 3$ and $n = 4$ with S as indicated. Transitions that are allowed by the selection rules are indicated. Thick line: GS–GS transition.

the missing of the linear conductance peak corresponding to the transition between the GSs with $n = 4$ and $n = 5$, and with $S = 0$ and $S = 3/2$, respectively. Either finite V or finite T can reestablish the conductance via transport through excited states with spins $S = 1$ $(n = 4)$ and/or $S = 1/2$ $(n = 5)$. The effect of V can be observed in Fig. 5(left). The T–induced recovery of the conductance is shown in Fig. 5(right). Such an effect was indeed experimentally observed [9]. Since in 1D the spins of the GSs are always 0 or 1/2, due to the Lieb and Mattis theorem [28], 'spin blockade type II' can only occur in 2D or 3D quantum dots. In a 'slim' dot no linear conductance peak should be missing.

Furthermore, states with high spins, but not necessarily completely polarized, which are energetically situated close to the GS, can cause blocking effects, and lead to NDCs close to a linear conductance peak. This is shown for the transition between $n = 3$ and $n = 4$ in Fig. 6(top), where the $(n = 3, S = 3/2)$–state **b** is almost degenerate with the $S = 1/2$ GS.

The levels that are most important for the transport are shown schematically in Fig. 6(bottom right). Within the Coulomb blockade region all transition rates that increase n are exponentially small. At $V = 0$ the system is in thermal equilibrium and the 3–electron GS populated. Even only a slight increase of V changes the ratio between certain rates by orders of magnitude, and favors the occupation of the $S = 3/2$ state **b** (Fig. 6(top right)). This is due to a delicate interplay between multiple transitions that connect eventually the lowest $n = 3$ states via several intermediate states. There is a competition between processes like $\mathbf{a} \rightarrow \mathbf{d} \rightarrow \mathbf{c} \rightarrow \mathbf{e} \rightarrow \mathbf{b}$ and $\mathbf{b} \rightarrow \mathbf{e} \rightarrow \mathbf{a}$. The direct transition $\mathbf{b} \rightarrow \mathbf{d}$ is spin forbidden which causes the pronounced NDC at low V.

To simulate the situation in a rectangular dot, we enhance slightly the energy of the lowest $(n = 3, S = 3/2)$–state **b**. Fig. 6(bottom) shows the differential conductance. NDC occurs now at voltages that depend on the excitation energy of the $(n = 3, S = 3/2)$–state **b**. When **b** starts to contribute to the transport, it attracts a large portion of the population at the expense of the GS **a**. This suppresses the GS–GS transition. Only for even higher V the $S = 3/2$–state can again be depopulated and the line corresponding to transitions involving the GSs is recovered. Features like this can also be seen in the greyscale plots of experimental results [6, 12].

6. Summary

We have investigated the non–linear transport through quantum dots that are weakly coupled to reservoirs taking into account Coulomb interactions, spin, and non–equilibrium effects. The calculations were carried out in the region where charging and geometrical quantization effects coexist. For different models, the current was calculated as a function of the transport– and the gate–voltage using a master equation.

Consistent with previous studies we find additional steps in the Coulomb staircase corresponding to transitions involving excited levels when the temperature is lower and the voltage higher than the excitation energies. Taking into account the quantum mechanics of Coulombically interacting electrons with spin, we have demonstrated that spin selection rules together with correlation effects can strongly influence the transport properties of semiconducting quantum dots. They lead to a spin blockade effect and explain in a natural way various of the experimentally observed features.

We have proposed two qualitatively different types of spin blockades. They influence the heights of the linear conductance peaks and lead to non–linear negative differential conductances. While 'spin blockade type I' is connected with highly excited spin–polarized states, 'spin blockade type II' is more general. It leads to qualitative changes even in linear transport, and is especially important for 2D systems.

All of the features predicted above are qualitatively consistent with experiments [4, 5, 6, 7, 8, 9, 10, 11, 12]. Also the effects of a magnetic field [16] are consistent with experimental findings [11, 12]. Thus, the spin blockade is very likely to be the physical mechanism behind at least some of the observed NDCs. Further experiments, in particular using 'slim quantum dots', are however necessary in order to clarify the quantitative aspects.

In experimental situations where the total spin of the electrons in the dot is not stable over long enough time scales, the spin blockade is expected to disappear. Introducing an inhomogeneous magnetic field in the dot region by using type II superconductors on top of the structure or doping the sample with magnetic impurities could confirm unambiguously the relevance of the spin blockade mechanism for transport. Such experiments are highly desirable and can in principle be carried out [29].

ACKNOWLEDGEMENTS

We thank T. Brandes, P. Hänggi, R. Haug, W. Pfaff, J. Weis, U. Weiss and D. Wharam for discussions. Part of this work was done at the PTB Braunschweig. Financial support of the DFG via grant We 1124/4–1 and from the EU by grant SCC*–CT90–0020 and by grant CHRX–CT93–0136, is gratefully acknowledged.

References

1. M. A. Kastner, *Physics Today*, p. 24 (January 1993).
2. Special Issue on *Single Charge Tunneling* edited by H. Grabert, *Z. Phys.* **B 85**, 317–468 (1991).
3. U. Meirav, M. A. Kastner, S. J. Wind, *Phys. Rev. Lett.* **65**, 771 (1990); L. P. Kouwenhoven, N. C. van der Vaart, A. T. Johnson, W. Kool, C. J. P. M. Harmans, J. G. Williamson, A. A. M. Staring, C. T. Foxon, *Z. Phys.* **B 85**, 367 (1991); M. A. Kastner, *Rev. Mod. Phys.* **64**, 849 (1992); T. Heinzel, S. Manus, D. A. Wharam, J. P. Kotthaus, G. Böhm, W. Klein, G. Tränkle, G. Weimann, *Europhys. Lett.* **26**, 689 (1994).
4. J. Weis, R. J. Haug, K. v. Klitzing, K. Ploog, *Phys. Rev.* **B 46**, 12837 (1992).
5. A. T. Johnson, L. P. Kouwenhoven, W. de Jong, N. C. van der Vaart, C. J. P. M. Harmans, C. T. Foxon, *Phys. Rev. Lett.* **69**, 1592 (1992).
6. J. Weis, R. J. Haug, K. v. Klitzing, K. Ploog, *Phys. Rev. Lett.* **71**, 4019 (1993).
7. N. C. van der Vaart, A. T. Johnson, L. P. Kouwenhoven, D. J. Maas, W. de Jong, M. P. de Ruyter van Stevenick, A. van der Enden, C. J. P. M. Harmans, *Physica* **B 189**, 99 (1993).
8. J. Weis, R. J. Haug, K. v. Klitzing, K. Ploog, *Physica* **B 189**, 111 (1993).

9. J. T Nicholls, J. E. F. Frost, M. Pepper, D. A. Ritchie, M. P. Grimshaw, G. A. C. Jones, *Phys. Rev.* **B 48**, 8866 (1993).
10. E. B. Foxman, P. L. McEuen, U. Meirav, N. S. Wingreen, Y. Meir, P. A. Belk, N. R. Belk, M. A. Kastner, S. J. Wind, *Phys. Rev.* **B 47**, 10020 (1993); P. L. McEuen, N. S. Wingreen, E. B. Foxman, J. Kinaret, U. Meirav, M. A. Kastner, Y. Meir, S. J. Wind, *Physica* **B 189**, 70 (1993).
11. J. Weis, R. Haug, K. v. Klitzing, K. Ploog, *Surf. Sci.* **305**, 664 (1994).
12. J. Weis, *Ph. D. Thesis*, Stuttgart (1994).
13. D. Weinmann, W. Häusler, W. Pfaff, B. Kramer, U. Weiss, *Europhys. Lett.* **26**, 467 (1994).
14. W. Pfaff, D. Weinmann, W. Häusler, B. Kramer, U. Weiss, *Z. Phys.* **B**, in press (1994).
15. D. Weinmann, W. Häusler, B. Kramer, preprint (1994).
16. D. Weinmann, Ph. D. thesis, Universität Hamburg (1994).
17. W. Häusler, K. Jauregui, D. Weinmann, T. Brandes, B. Kramer, *Physica* **B 194-196**, 1325 (1994).
18. U. Weiss, *Quantum Dissipative Systems* (World Scientific, Singapore, 1993).
19. J. M. Kinaret, Y. Meir, N. S. Wingreen, P. A. Lee, X.-G. Wen, *Phys. Rev.* **B 46**, 4681 (1992).
20. C. W. J. Beenakker, *Phys. Rev.* **B 44**, 1646 (1991).
21. D. V. Averin, A. N. Korotkov, *Journ. of Low Temp. Phys.* **80**, 173 (1990); D. V. Averin, A. N. Korotkov, K. K. Likharev, *Phys. Rev.* **B 44**, 6199 (1991).
22. D. V. Averin, A. A. Odintsov, *Phys. Lett.* **A 140**, 251 (1989); D. V. Averin, Yu. V. Nazarov in *Single Charge Tunneling*, ed. by H. Grabert, M. H. Devoret (Plenum, New York, 1991).
23. W. Häusler, B. Kramer, J. Mašek, *Z. Phys.* **B 85**, 435 (1991); W. Häusler, B. Kramer, *Phys. Rev.* **B 47**, 16353 (1993); T. Brandes, W. Häusler, K. Jauregui, B. Kramer, D. Weinmann, *Physica* **B 189**, 16 (1993).
24. W. Häusler, preprint (1994).
25. K. Jauregui, W. Häusler, B. Kramer, *Europhys. Lett.* **24**, 581 (1993).
26. K. Jauregui, unpublished (1994).
27. D. Pfannkuche, private communication (1994).
28. E. Lieb, D. Mattis, *Phys. Rev.* **125**, 164 (1962).
29. D. A. Wharam, private communication (1994).